

Molecular Hysteresis in a Rigid Dinuclear Ruthenium Polypyridyl Complex Incorporating a Ligand-Bound Ambidentate Motif

Olof Johansson* and Reiner Lomoth*

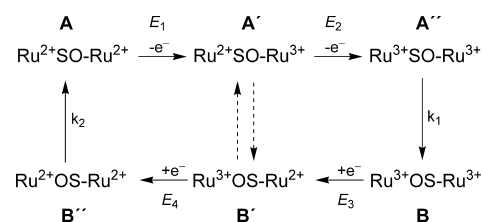
Department of Photochemistry and Molecular Science, Uppsala University, Box 523, 751 20 Uppsala, Sweden

Received January 15, 2008

Two alternative $\text{Ru}_2^{2+/3+}$ mixed-valence states are formed in the first dinuclear Ru complex with a ligand-bound ambidentate motif. The hysteretic electrochemical response follows a double-square scheme where the structure of the mixed-valence state depends on the previous isovalent state. The Ru^{3+} state of the pyrrolidine-substituted bisterpyridine unit is characterized by intense ligand-to-metal charge-transfer absorptions that provide a distinctive signature of the corresponding mixed-valence state.

Bistable molecules with the ability to persist in two states at the same value of an external parameter are interesting candidates as molecular memories.¹ An important class of molecules that show this behavior is coordination compounds that undergo electrochemically induced linkage isomerism or other reversible structural changes.^{2–4} The sequence of alternating electron-transfer (E) and chemical (C) steps follows a square scheme, also referred to as an ECEC mechanism. The electrochemical response is then characterized by the fact that the potentials for the metal-centered

Scheme 1



redox process can be largely different for the two isomers.⁵ As a consequence, the oxidation state of the system at any intermediate potential will depend on the electrochemical history, which can be considered as a form of hysteresis on the single-molecule level.^{3d} Paradigms of such behavior are Ru complexes based on sulfoxide ligands,² e.g., $[\text{Ru}(\text{NH}_3)_5(\text{sulfoxide})]^{2+}$, where the ambidentate sulfoxide ligand is S-bound to Ru^{2+} but isomerizes upon metal oxidation, and Cu-based complexes that show monomer/dimer interconversions.³ However, in the narrower definition of molecular hysteresis introduced by Sano and Taube, the system must not differ in composition in the two states⁶ including total charge and counterions. For this purpose, they elegantly combined a $[\text{RuL}_5(\text{sulfoxide})]^{2+}$ unit with a second Ru complex that features a reversible $\text{Ru}^{3+/2+}$ couple in between the potentials of the two isomers of the ruthenium sulfoxide motif.^{6,7} The redox behavior of these dinuclear complexes can be illustrated in a double-square scheme (Scheme 1). The complexes can exist in either of two mixed-valence states, A' and B', that are accessible by oxidation of the fully reduced form (A) or reduction of the fully oxidized form (B), respectively. The mixed-valence states remember their former structures, and which state is present depends on the direction of the applied potential change.

* To whom correspondence should be addressed. E-mail: olof.johansson@fotomol.uu.se (O.J.), reiner.lomoth@fotomol.uu.se (R.L.).

- (1) (a) Kahn, O.; Launay, J.-P. *Chemtronics* **1988**, *3*, 140–151. (b) Kölle, U. *Angew. Chem., Int. Ed.* **1991**, *30*, 956–958.
 (2) (a) Yeh, A.; Scott, N.; Taube, H. *Inorg. Chem.* **1982**, *21*, 2542–2545. (b) Tomita, A.; Sano, M. *Inorg. Chem.* **1994**, *33*, 5825–5830. (c) Rack, J. J.; Winkler, J. R.; Gray, H. B. *J. Am. Chem. Soc.* **2001**, *123*, 2432–2433. (d) Sens, C.; Rodríguez, M.; Romero, I.; Llobet, A.; Parella, T.; Sullivan, B. P.; Benet-Buchholz, J. *Inorg. Chem.* **2003**, *42*, 2040–2048. (e) Rachford, A. A.; Petersen, J. L.; Rack, J. J. *Inorg. Chem.* **2005**, *44*, 8065–8075.
 (3) (a) Potts, K. T.; Keshavarz-K, M.; Tham, F. S.; Abruña, H. D.; Arana, C. R. *Inorg. Chem.* **1993**, *32*, 4422–4435. (b) Amendola, V.; Fabbri, L.; Linati, L.; Mangano, C.; Pallavicini, P.; Pedrazzini, V.; Zema, M. *Chem.—Eur. J.* **1999**, *5*, 3679–3688. (c) Amendola, V.; Fabbri, L.; Gianelli, L.; Maggi, C.; Mangano, C.; Pallavicini, P.; Zema, M. *Inorg. Chem.* **2001**, *40*, 3579–3587. (d) Amendola, V.; Fabbri, L.; Pallavicini, P. *Coord. Chem. Rev.* **2001**, *216–217*, 435–448. (e) Amendola, V.; Mangano, C.; Pallavicini, P.; Zema, M. *Inorg. Chem.* **2003**, *42*, 6056–6062.
 (4) (a) Sauvage, J.-P. *Acc. Chem. Res.* **1998**, *31*, 611–619. (b) Poleschak, I.; Kern, J.-M.; Sauvage, J.-P. *Chem. Commun.* **2004**, 474–476. (c) Létinois-Halbes, U.; Hanss, D.; Beierle, J. M.; Collin, J.-P.; Sauvage, J.-P. *Org. Lett.* **2005**, *7*, 5753–5756. (d) Durola, F.; Sauvage, J.-P. *Angew. Chem., Int. Ed.* **2007**, *46*, 3537–3540.

- (5) Cyclic voltammograms of these systems are characterized by a major displacement of an oxidation peak and the corresponding reduction peak.
 (6) Sano, M. Molecular Hysteresis by Linkage Isomerizations Induced by Electrochemical Processes. In *Molecular Machines and Motors*; Sauvage, J.-P., Ed.; Springer-Verlag: Berlin, 2001; pp 117–139.
 (7) (a) Sano, M.; Taube, H. *J. Am. Chem. Soc.* **1991**, *113*, 2327–2328. (b) Sano, M.; Taube, H. *Inorg. Chem.* **1994**, *33*, 705–709. (c) Tomita, A.; Sano, M. *Chem. Lett.* **1996**, 981–982. (d) Tomita, A.; Sano, M. *Inorg. Chem.* **2000**, *39*, 200–205.

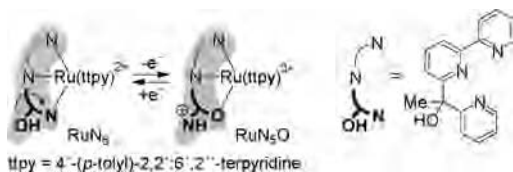
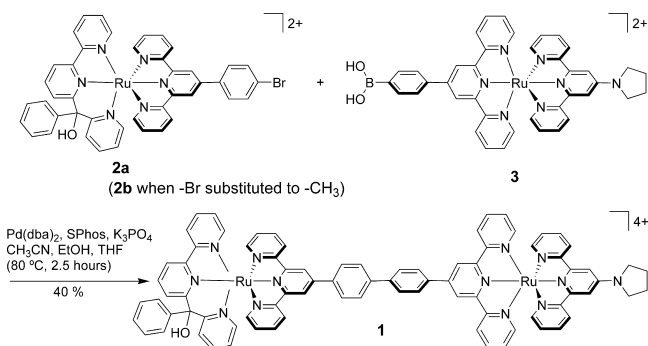


Figure 1. Electron-transfer-induced isomerization of a ligand-bound ambidentate motif.

Scheme 2



We recently reported a bistable ruthenium polypyridyl complex with a ligand-bound ambidentate motif that undergoes reversible redox-induced linkage isomerization (Figure 1).⁸ As the major novelty, the tridentate ligand ensures chemical stability to the Ru complex when switching between the N_6 and N_5O isomers. In view of their electrochromic properties, these complexes could be ideal building blocks for a new family of dinuclear complexes that feature molecular hysteresis according to Scheme 1. In particular, we anticipated that judicious substitution of the ligands could result in distinct absorption features of the two mixed-valence states for the purpose of reading the memory of the system. Here we present the first example of a dinuclear Ru complex (**1**) based on our ambidentate motif and report its basic electrochemical and electrochromic characteristics.

As the bistable unit, a Ru complex based on the ligand (2,2'-bipyridin-6-yl)phenyl(pyridin-2-yl)methanol was used where the phenyl substituent was expected to reduce isomerization rates compared to the previously studied methyl analogue. As the nonbistable unit, a pyrrolidine-containing Ru complex was chosen because of the suitable potential of its $Ru^{3+/2+}$ couple and the expected spectroscopic signature of the Ru^{3+} state.⁹ The synthesis of **1** relied on a Suzuki–Miyaura cross-coupling of the appropriately functionalized Ru precursors **2a** and **3** (Scheme 2). Refluxing **2a** and **3** in a $CH_3CN/EtOH/THF$ mixture with $Pd(dba)_2/SPhos$ (1:2, 6 mol % Pd to boronic acid) and K_3PO_4 gave complex **1** in 40% isolated yield after column chromatography on silica and a subsequent recrystallization (Supporting Information). The resulting biphenyl linker is expected to result in weak metal–metal interaction, as has been shown in other dinuclear ruthenium polypyridyl complexes.¹⁰

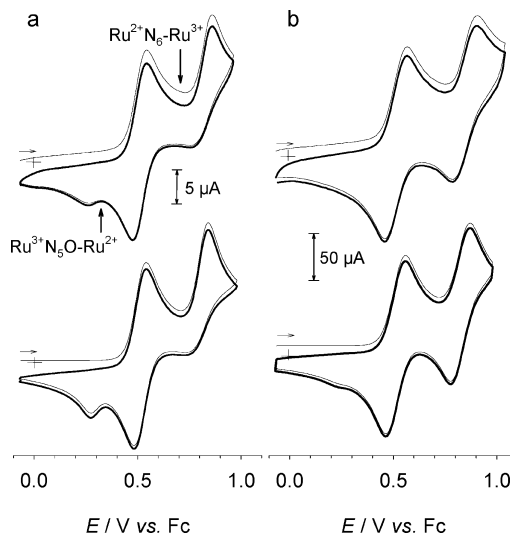
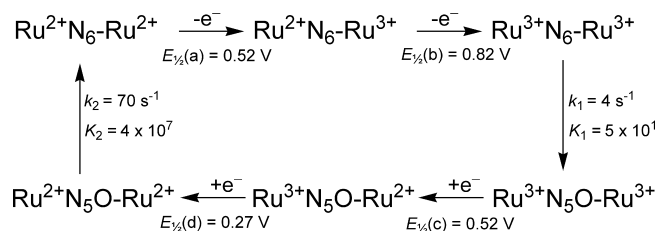


Figure 2. Cyclic voltammograms (top) and digital simulations (bottom) of **1** (0.75 mM) in CH_3CN with $\nu = 0.100 \text{ V s}^{-1}$ (a) and 5.00 V s^{-1} (b). Simulation parameters according to Scheme 3 and $k_{com} = 1 \times 10^6 \text{ M}^{-1} \text{ s}^{-1}$.

Scheme 3



In the cyclic voltammogram of **1** (Figure 2), a reversible wave is observed at $E_{1/2} = 0.52 \text{ V}$ ($\Delta E_p = 70 \text{ mV}$)¹¹ (vs $Fc^{+/0}$) that can be assigned to the $Ru^{3+/2+}$ redox couple of the pyrrolidine-substituted unit ($Ru^{2+}N_6-Ru^{3+/2+}$).¹² At low scan rates (0.1 V s^{-1}), an anodic wave at $E_{p,a} = 0.86 \text{ V}$ is observed with no corresponding reduction wave on the reverse scan (Figure 2a).

In analogy to our previous results, we ascribe this behavior to an isomerization of the bistable unit to the oxygen-coordinated form ($Ru^{3+}N_6-Ru^{3+} \rightarrow Ru^{3+}N_5O-Ru^{3+}$).⁸ On the reverse scan, the reduction of the pyrrolidine-substituted unit ($Ru^{3+}N_5O-Ru^{3+/2+}$) instead precedes an irreversible cathodic peak at 0.25 V due to reduction of the oxygen-coordinated Ru ($Ru^{3+/2+}N_5O-Ru^{2+}$). The corresponding oxidation peak is not observed on subsequent scanning because of rapid re-isomerization in the Ru^{2+} state ($Ru^{2+}N_5O-Ru^{2+} \rightarrow Ru^{2+}N_6-Ru^{2+}$). Only at higher sweep rates ($\nu \geq 1 \text{ V s}^{-1}$), the reverse peak at $E_{p,c} = 0.80 \text{ V}$ starts to appear, and at 5 V s^{-1} the rereduction completely outcompetes the isomerization (Figure 2b). The voltammograms of **1** could be reproduced by digital simulations (Figure 2) with the square scheme parameters shown in Scheme 3.

- (11) Formally the peaks of the reversible wave arise from two different redox couples ($Ru^{2+}N_6-Ru^{3+/2+}$ and $Ru^{3+}N_5O-Ru^{3+/2+}$). Because of the very weak electronic coupling between the metal centers, their standard potentials are basically identical ($E_{1/2}(a) = E_{1/2}(c)$).
- (12) The assignment is based on a comparison to the mononuclear complex **3** with $E_{1/2} = 0.52 \text{ V}$. A similar value (0.58 V vs $Fc^{+/0}$) has been reported for $[Ru(NMe_2tpy)(tpy)]^{2+}$. Constable et al. *New J. Chem.* **1992**, *16*, 855–867.

(8) Johansson, O.; Lomoth, R. *Chem. Commun.* **2005**, 1578–1580.

(9) [(4-Aminopyridine)Ru(NH₃)₅]³⁺ shows pronounced ligand-to-metal charge-transfer transitions due to the donor properties of the pyridyl ligand. Sutton, J. E.; Taube, H. *Inorg. Chem.* **1981**, *20*, 4021–4023.

(10) Collin, J.-P.; Lainé, P.; Launay, J.-P.; Sauvage, J.-P.; Sour, A. *J. Chem. Soc., Chem. Commun.* **1993**, 434–435.

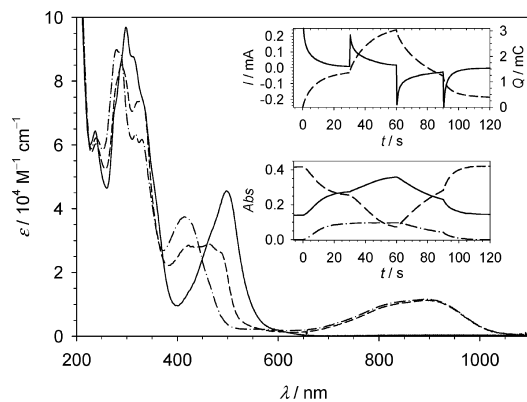
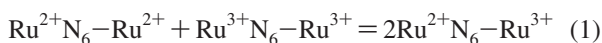


Figure 3. Electronic absorption spectra of $\text{Ru}^{2+}\text{N}_6\text{-Ru}^{2+}$ (—), $\text{Ru}^{2+}\text{N}_6\text{-Ru}^{3+}$ (---), and $\text{Ru}^{3+}\text{N}_5\text{O-Ru}^{3+}$ (- · -) in CH_3CN with 0.1 M $[(n\text{-C}_4\text{H}_9)_4\text{N}][\text{PF}_6]$. The latter were obtained after exhaustive electrolysis at 0.62 and 0.87 V. Insets: Current (—) and charge (---) passed through the spectroelectrochemical cell (top) and induced absorbance changes (bottom) at 420 (—), 490 (---), and 900 (- · -) nm after potential steps to 0.62 (from open circuit, $t = 0$ s), 0.87 ($t = 30$ s), 0.45 ($t = 60$ s), and -0.08 ($t = 90$ s) V.

These are identical with the potentials and isomerization parameters of the mononuclear complexes **2b** and **3**, which supports the notion of weak electronic communication between the two units of **1**.¹³ Simulations had, however, to include a bimolecular disproportionation reaction between $\text{Ru}^{3+}\text{N}_6\text{-Ru}^{3+}$ formed at the electrode and $\text{Ru}^{2+}\text{N}_6\text{-Ru}^{2+}$ in the bulk solution (eq 1). Reaction 1 is thermodynamically strongly favored ($K_{\text{com}} = \exp[\Delta E_{1/2}F/RT] = 1.2 \times 10^5$, at 298 K) and results in the observed depletion of the reduction peak for $\text{Ru}^{3+}\text{N}_5\text{O-Ru}^{2+}$ at ca. 0.3 V when included in the simulations with $k_{\text{com}} \geq 10^6 \text{ M}^{-1} \text{ s}^{-1}$.¹⁴



As indicated in Figure 2a, the voltammetric data demonstrate that two different mixed-valence states are accessible, either by oxidation of the fully reduced form or by reduction of the fully oxidized form (Scheme 3). In between the indicated potentials, the structure of the complex is therefore dependent on the previous redox state. In this sense, the electrochemical response of **1** represents an example of molecular hysteresis.

The electronic absorption spectrum of **1** (Figure 3) shows intense metal-to-ligand charge-transfer absorptions in the visible that arise from the two Ru^{2+} units. The contribution from the pyrrolidine-substituted unit is bleached upon oxidation at 0.62 V, and the resulting $\text{Ru}^{2+}\text{N}_6\text{-Ru}^{3+}$ shows

distinct and intense absorptions in the red and near-infrared. These features are unaffected by further oxidation to the iso-valent $\text{Ru}^{3+}\text{N}_5\text{O-Ru}^{3+}$ state at 0.87 V, which proves that the low-energy transitions have no intervalence character but are intrinsic to the pyrrolidine-substituted Ru^{3+} .⁹ Because these absorptions do not overlap with any features of the bistable unit, they should provide a discrete (on/off) read-out signal that discriminates the two mixed-valence states.

To observe the absorption spectrum of the alternative $\text{Ru}^{3+}\text{N}_5\text{O-Ru}^{2+}$ state, a sequence of potential steps was applied to a spectroelectrochemical thin layer cell (insets in Figure 3). The first two steps generated $\text{Ru}^{2+}\text{N}_6\text{-Ru}^{3+}$ and subsequently $\text{Ru}^{3+}\text{N}_5\text{O-Ru}^{3+}$, while a third step was supposed to generate $\text{Ru}^{3+}\text{N}_5\text{O-Ru}^{2+}$ by reduction of the fully oxidized state. The coulometric data showed, however, that more than one electron per complex is transferred at the potential of the third step, which precludes clean conversion into $\text{Ru}^{3+}\text{N}_5\text{O-Ru}^{2+}$. Instead, the associated spectroscopic changes indicated the formation of $\text{Ru}^{2+}\text{N}_6\text{-Ru}^{2+}$ already at the potential of the third step. This behavior can be rationalized if it is assumed that $\text{Ru}^{3+}\text{N}_5\text{O-Ru}^{2+}$ undergoes further transformation more rapidly than can be generated by electrolysis in the spectroelectrochemical cell that has a diffusion-limited time constant of about 20 s. Transformation of $\text{Ru}^{3+}\text{N}_5\text{O-Ru}^{2+}$ into $\text{Ru}^{2+}\text{N}_5\text{O-Ru}^{2+}$ at the electrode or by disproportionation is disfavored with the electrode potential well above $E_{1/2}(\text{d})$ and $K_{\text{dis}} = 4.5 \times 10^{-5}$ (at 298 K). The subsequent isomerization to $\text{Ru}^{2+}\text{N}_6\text{-Ru}^{2+}$ shifts these equilibria, however, to the product side and thereby enables conversion of $\text{Ru}^{3+}\text{N}_5\text{O-Ru}^{3+}$ to $\text{Ru}^{2+}\text{N}_6\text{-Ru}^{2+}$ already at electrode potentials $E_{1/2}(\text{c}) > E > E_{1/2}(\text{d})$.

In summary, we have shown that the ligand-bound ambidentate motif can be incorporated in dinuclear assemblies where the potentials for the three metal-centered electron-transfer reactions are chosen to result in a double-square scheme behavior according to Sano's definition of molecular hysteresis. Furthermore, we could demonstrate that units with largely different electrochromic responses can be combined in a way that ensures unique spectroscopic signatures of the two alternative mixed-valence states that are much more distinct than the rather similar mixed-valence bands reported for earlier systems.

Future work will be directed toward immobilization of the complexes, which will allow for rapid electrochemical addressing without the limitations arising from diffusional mass transport and bimolecular reactions.

Acknowledgment. This work was financially supported by the Swedish Energy Agency, the Knut and Alice Wallenberg Foundation, the Carl Trygger Foundation, and NEST-STRP, SOLAR-H (EU Contract 516510).

Supporting Information Available: Experimental details and characterizations for complexes **1**, **2a**, **2b**, and **3**, ¹H NMR and mass spectra of **1**, cyclic voltammograms, and simulations. This material is available free of charge via the Internet at <http://pubs.acs.org>.

IC800075B

(13) Note that the phenyl moiety of the ambidentate ligand reduces the isomerization rates compared to the millisecond kinetics observed for the methyl analogue.⁸

(14) Alternatively, transformation of $\text{Ru}^{3+}\text{N}_5\text{O-Ru}^{2+}$ into $\text{Ru}^{2+}\text{N}_6\text{-Ru}^{3+}$ could also account for the depleted reduction peak in **1**. Such short-cut reactions between the mixed-valence states (Scheme 1) have been reported for similar systems (see, e.g., Harman, W. D.; Taube, H. *J. Am. Chem. Soc.* **1988**, *110*, 5403–5407. Sano, M.; Sago, H.; Tomita, A. *Bull. Chem. Soc. Jpn.* **1996**, *69*, 977–981). The analogous behavior of equimolar mixtures of **2b** and **3** and the better agreement of isomerization parameters for **1** and **2b** (Supporting Information) indicate, however, that the voltammograms of complex **1** are more readily rationalized on the basis of the comproportionation reaction (eq 1).